《原 著》

Processing Data from Scintillation Camera Using a Minicomputer

—A Study of the Heart Scintigram Functional Image Using an ECG-Gate—

Takeo HASEGAWA*, Kiyoshi AKAGI*, Hiroshi HASHIBA*, Akitoshi KOBAYASHI*, Magoichi MATSUDA* and Tsukasa SHIMOGAMA**

*Department of Radiology, Kansai Medical University
**System Engineering, Toshiba Medical Co.

Abstract There has been much progress in minicomputers in recent years, allowing extensive analysis of the RI image using scintillation camera. Using a TOSBAC-10E (HOSPICON-600: Toshiba), Anger-type scintillation camera and LAB system (Toshiba), we conducted a functional image analysis of the heart and RI image processing with this study. Taking patients who came for RI examinations as subjects, Tc-99m (10–20 mCi) was rapidly injected by bolus through the anticubital vein. Data from the scintillation camera was processed by the minicomputer and collected in list mode from the time of injection in intervals ranging from 10 to 100 msec. A sample interval was selected by use of ECG gating. The gate is triggered after an arbitrary time lag following the detection of the R-wave, and the ECG wave was stored together with the image data in a magnetic disk. When the image was reproduced, it was displayed together with its corresponding ECG wave on the CRT. Further processing of the reproduced image was easily accomplished using the minicomputer. The possible types of such processing and derivable information include the following: ROI (region of interest) designation and the functional curve display of the ROI, superimposing images, stroke volume calculation, heart wall movement display, level cutting, smoothing, oblique display, and profile display. The following is a report on the results of a functional analysis of the heart using the software mentioned above.

I. Introduction

Owing to the development of software for medical use of the minicomputer, RI image analysis using the minicomputer in combination with a scintillation camera has become wide-spread[1~8]. In order to conduct a functional image analysis of the heart, and ECG was set up on a reclining patient, and Tc-99m (10–20 mCi) was rapidly injected through the anticubital vein. Data from the scintillation camera was collected from the time of injection in either list mode or map mode, and was stored together in the magnetic disk with the position signal of the scintillation camera and the ECG signal. The image was reproduced using an on-line typewriter, conditions being entered in a conversational format allowing free choice of time and reproduction intervals. When reproducing the image, the ECG wave is displayed to the right or below the image, and by displaying a point on the ECG wave, the movement of the heart in relation to the ECG can be seen. Up to four channels of input on organ phenomena are possible. Single or four simultaneous image displays are possible. An image reproduced from data gathered in map mode allows profile display, oblique display, smoothing, level cutting and similar processing to be performed on the same image. With an image reproduced using data gathered in list mode, a gated image can be obtained, images corresponding to the same phase can be superimposed, and as with map mode data, the ECG wave can be displayed together with the image. Designating a ROI on these images, a diagram of the heart was

受付：54年2月19日
最終稿受付：54年11月5日
別刷請求先：守口市文園町1 (〠570)
関西医科大学放射線科
長谷川 武 夫

Presented by Medical*Online

made, the IO curve and similar results were obtained, and by analyzing these, E.F., heart wall movement, heart volume and its changes, and other heart functions were analyzed.

II. Equipment and procedure

1. Equipment

The following equipment was used in the study: Anger-type scintillation camera (GCA-202: Toshiba), storage display unit (Type 661: Tektronix), floppy disk (FDS-8: Toshiba), hard copy (Type 4610: Tektronix), minicomputer (HOSPICON-600: Toshiba), LAB system (Toshiba), collimator (1500H: Toshiba), phantom (home-built), γ-ray source (Tc-99m), A general view of the study is shown in photo-1, and the block diagram is shown in Fig. 1.

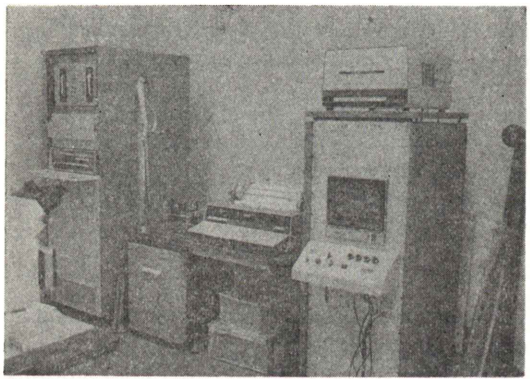

Photo. Minicomputer (HOSPICON-600) and LAB System used in this research.

2. Procedure

2-1) Data Gathering procedure

a) List Mode Gathering: Data is gathered in a 160×160 matrix, either in time base or in pulse base. Data can be collected in intervals ranging from 10 msec to 99 hours. Once begun, data collection continues until the disk is filled to capacity. It is possible to record up to four channels of organ waves simultaneously, and when only one channel is used for organ wave input, three separate triggers (ECG wave mark) can be entered using the heart monitor. The minicomputer (HOSPICON-600 and LAB system) contained two buffer areas in order to reduce deadtime while storing data in the disk from the core. The buffer areas were used alternately by an overlap process. While one of the buffers gathered the x, y, data signals as serial data from the scintillation camera, the data stored in the other buffer was sent to the disk. Thus, by alternating between gathering and sending data, deadtime while storing data in the disk was reduced. Since data gathered by list mode is stored in the disk as serial data, it has the advantage of producing the organ wave with its corresponding image, but the data cannot be used to display an image directly. The image can be obtained only by dividing the data (x_1y_1, x_2y_2, ...) into established time intervals, and arranging the divided data series in a 160×160 matrix. This time interval can be chosen in any length between 10 msec and 99 hours. The possible number of recorded images is determined by the counting rate of the scintillation camera.

b) Map Mode Gathering: Data is gathered

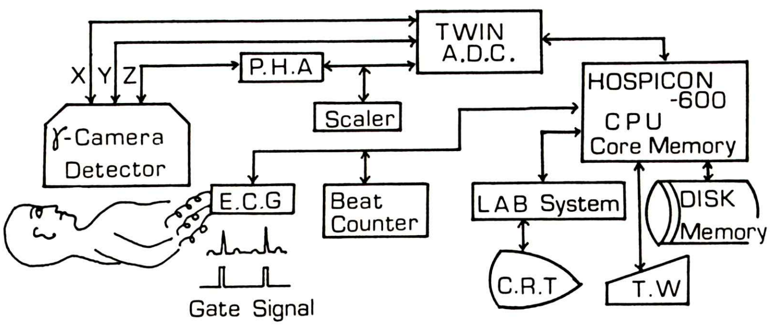

Fig. 1 Block diagram of the system. The gate signal seen in the diagram may be used to arbitrarily mark any phase of a beat-beat for the purpose of analysis after list mode data gathering has been performed.

Presented by Medical*Online

in a 64×64 or 128×128 matrix. The interval between images can be set anywhere between 10 msec and 99 hours. It is possible to collect up to 368 images with a 64×64 matrix, and up to 138 images using a 128×128 matrix. The advantage of this gathering method is that an area for the image is set up in the minicomputer from the beginning, enabling the creation of an image by arranging the data arriving from the scintillation camera into the area during a particular time interval. In contrast to list mode gathering, the collected data can be displayed as an image without any calculations. Two methods of data gathering are possible: pulse mode and time mode. The former is triggered by a gate using an instrument such as an ECG, and the image at the gate is collected. In the latter, images are collected at evenly spaced intervals.

3. Display Method

3–1) Display for List mode

There are two possible methods of display: 1) map mode, 2) ROI processing. When map mode processing is used, as many as 99 images can be superimposed and a display of either a 256×256, 128×128, or a 64×64 matrix is possible. The ECG wave is displayed together with the image on the CRT, and a point is inserted on the ECG wave indicating the phase depicted in the image (Fig. 2, Fig. 3). Total counts, maximum counts, the number of smoothings, etc., can also be displayed above the image. With the ROI process, an ap-

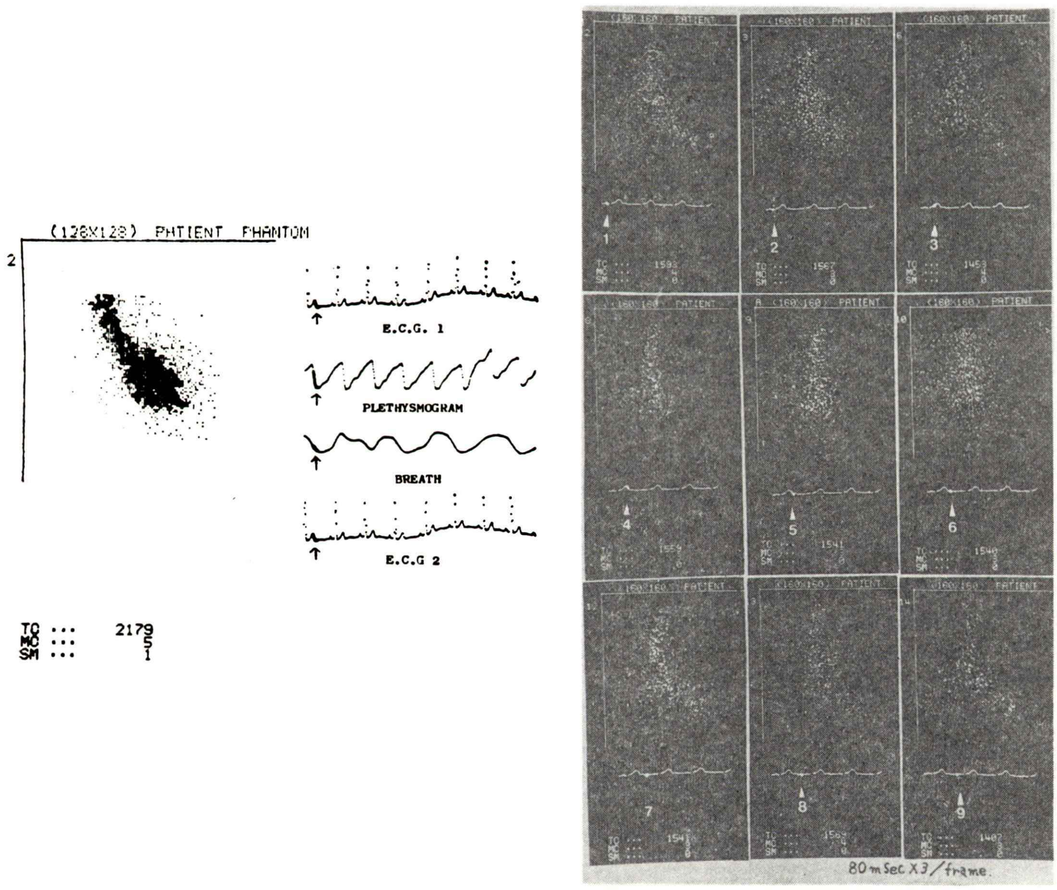

Fig. 2 Left: Left ventricule 128×128 matrix image and four channels indicating wave of the vital functions. (the left heart image corresponds to the indicated point on the wave of the vital functions).
Right: 80 msec 3 frame composite picture of the left ventricule in the same phase.

Presented by Medical*Online

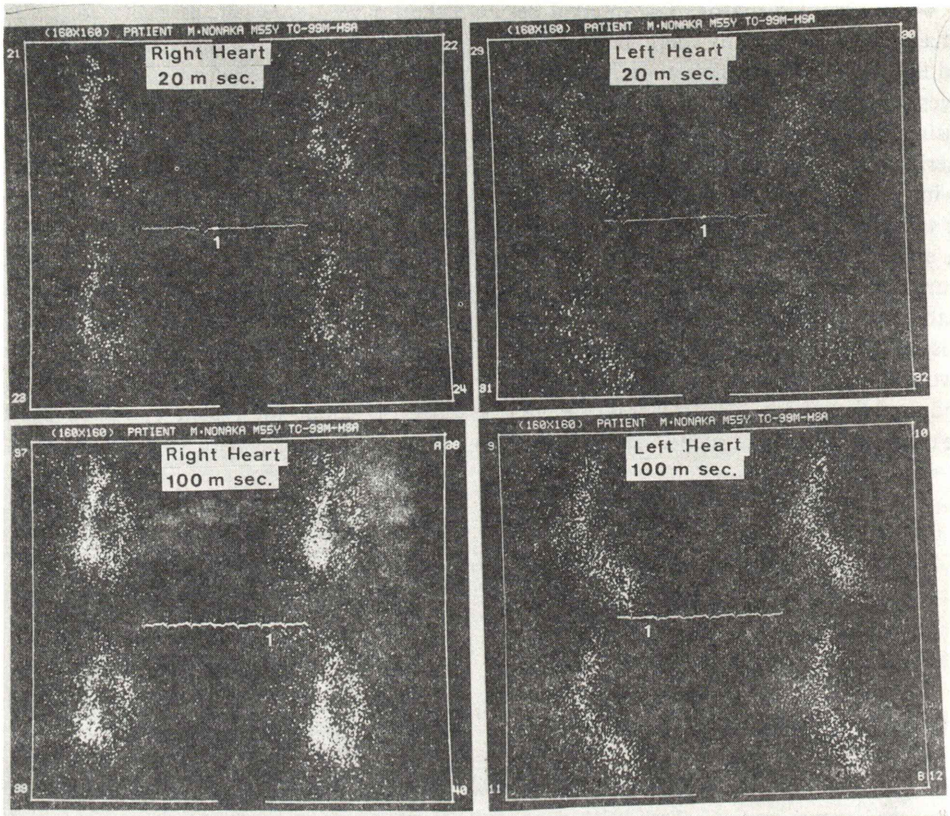

Fig. 3 Continuous 4 image displays of the right and left ventricules. (First images are taken at indicated points on the ECG wave, the following 3 images of each group are taken at indicated time intervals.)

propriate image is chosen, and while observing that image, a ROI is chosen using the potentiometer of the LAB system. (Four ROI's can be chosen at the same time.) The ROI can be subjected to background elimination, clearance (IG) curve processing, and volume (IO) curve processing. Fig. 4, Fig. 5, and Fig. 6 are displays of data gathered by list mode.

3–2) Display for Map Mode Gathering

Either 128×128 or 64×64 matrix displays are possible, and images can be readily superimposed with map mode gathering. Either single or four simultaneous image displays are possible. Using a single display, a profile display of the image or a 30° or 40° oblique display can be produced, and the image can be subjected to processing such as level cutting and smoothing.

III. Deadtime During Dynamic Studies

1. Elements of Deadtime

Generally, when the minicomputer is used for gathering data or for photographing highly concentrated radiation sources, the problem of deadtime arises.[19~24] The elements of deadtime can be roughly divided into deadtime in the scintillation camera, the conversion time of the twin A/D converter, load time into the core, and time to store data in the disk. Deadtime in the HOSPICON-600 system used in this study is as follows:

(a) Deadtime of the scintillation camera detector (Fig. 7).
(b) Conversion time in the twin ADC: 16 μsec.
(c) Core memory load time: 34 μsec. (16 μsec in the test program).

Presented by Medical*Online

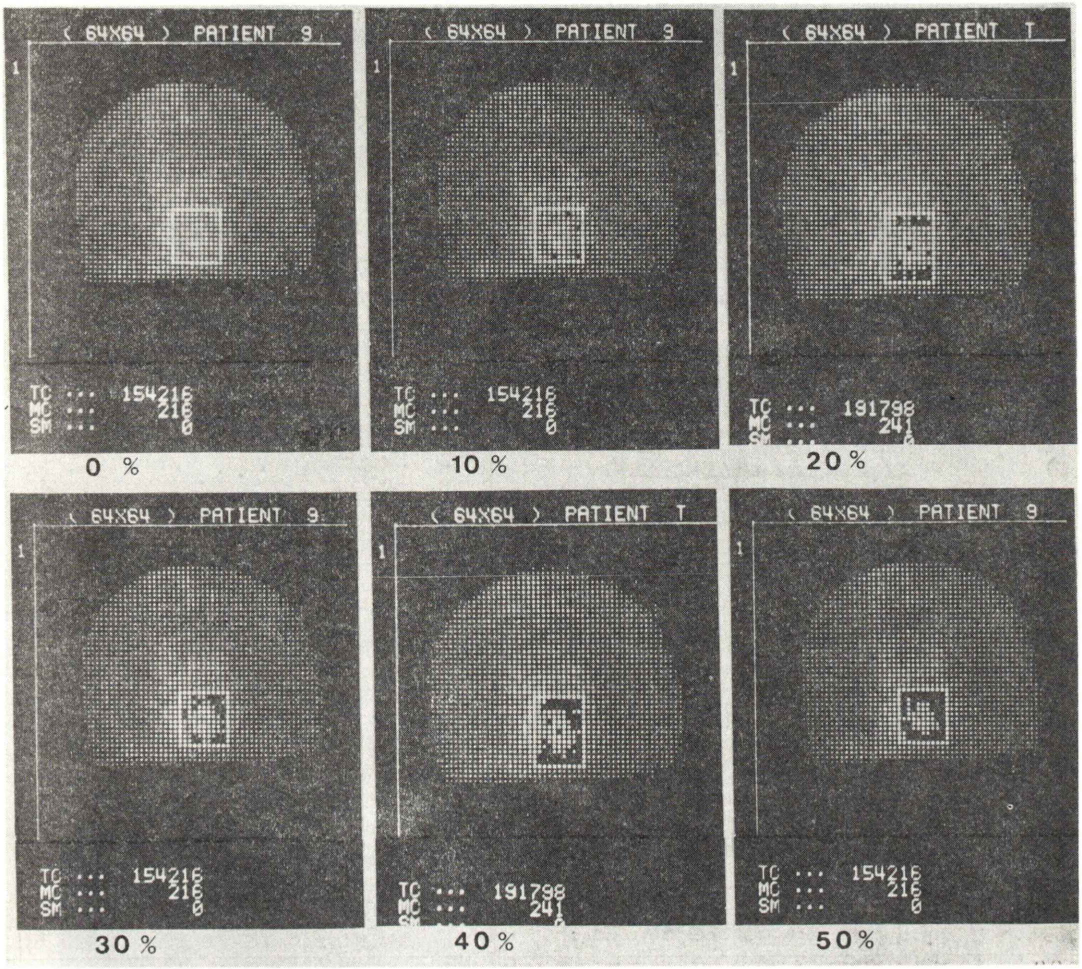

Fig. 4 Clear left ventricule image displays through background cutting. (The background cutting method entails selecting an area of interest, then applying lower level cuts.)

(d) Storing time in the disk: 60–80 msec.

(e) Disk access time: mean of approximately 14 msec.

The following equation gives a good approximation of deadtime in this system: $M/N=a/(1+N\tau)$, where M is the counting rate of the minicomputer, N is the counting rate derived from the scintillation camera scaler, τ is the sum of the deadtime during data conversion of the twin ADC (τ_t) and deadtime during core memory loading (τ_c), and (a) is the coefficient of data loss (the ratio to the area of the 160×160 matrix) determined by choice of the core area (256×256, 128×128, or 64×64). Fig. 7, and Fig. 8 compare theoretical deadtime and measured deadtime. The accuracy of the equation above can be easily observed.

IV. Results and Discussion

1. On Deadtime

Deadtime during data gathering with a scintillation camera and minicomputer is most affected by the size of the core, and then by the software system. Since the minicomputer used in this study was relatively small, having only 16K-B, a magnetic disk was used as a supplementary memory

Presented by Medical*Online

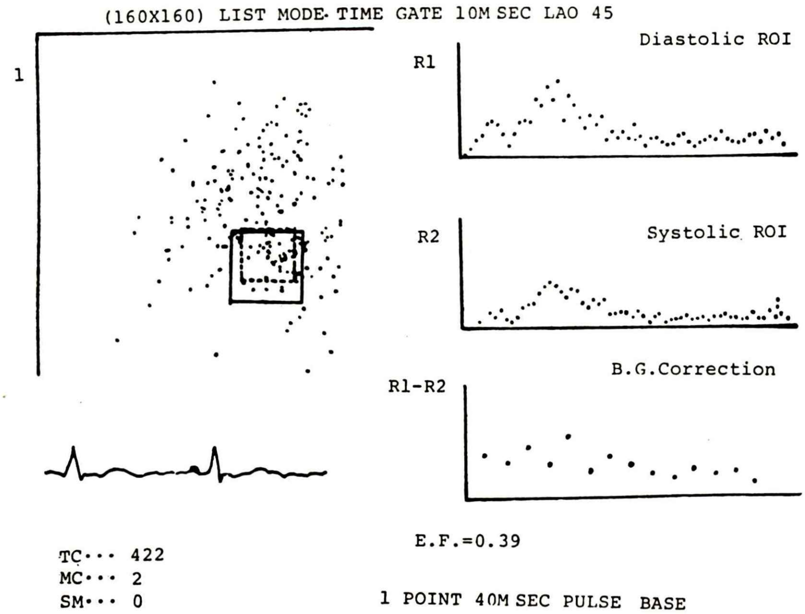

Fig. 5 Left: Display of left ventricule with indicated ROI and ECG.
Right: IG curve display.

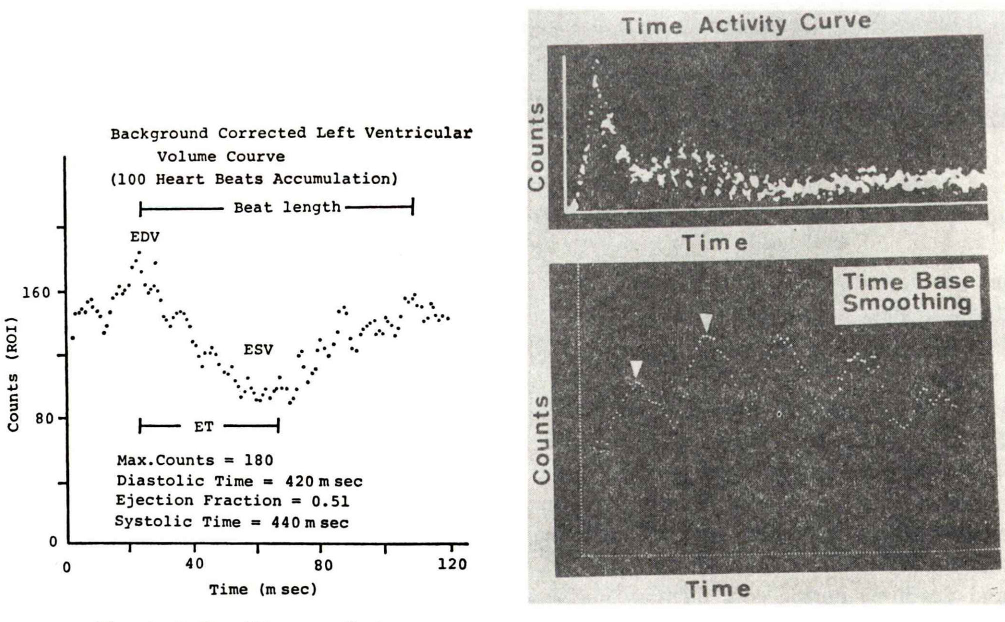

Fig. 6 Left: IO curve display.
Right: IG curve display. Above display image-point intraval is 100 msec.
Lower display image-point interval is 10 msec.

Presented by Medical*Online

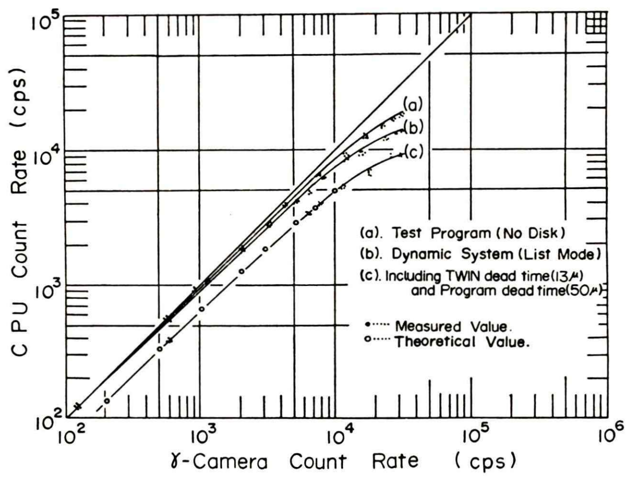

Fig. 7 Relation of computer count rate to γ-camera count rate.

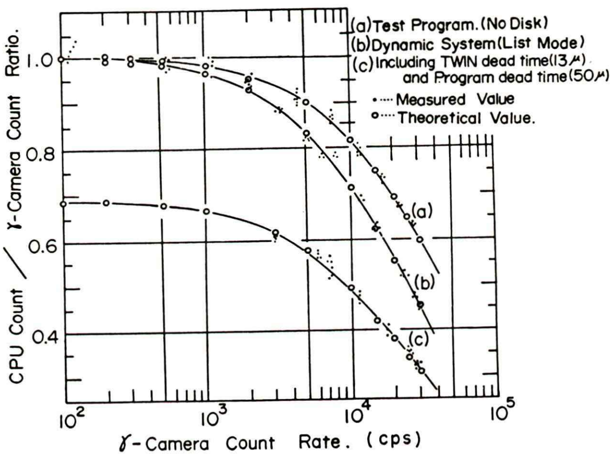

Fig. 8 Relation of computer count and γ-camera count ratio to γ-camera count rate.

device and the minicomputer core was divided into two buffer areas to be used alternately in order to minimize the number of data transmissions. (The first buffer collects data while data in the second buffer is being transmitted. When the first buffer is filled, the two areas switch functions). Reducing the number of data transmissions between the core and the disk in this way is one method of reducing deadtime. The deadtime in this study was 20μ sec for the test program, and 40μ sec for list mode. The data loss coefficient, "a" indicates the portion of area occupied by data in the 256×256 matrix. Since a 160×160 matrix was used in this study, "a" equaled 0.39. The size of each area was 6K-B (3072 counts), the maximum transmission time was 80 msec, and the number of data transmissions determined deadtime. It was found that if the core used was greater than 22K-B, deadtime would have been reduced greatly.

2. On the Image

Data gathered in either list mode or mp mode can be displayed in 256×256, 128×128 or 64×64 matrices, level cutting, smoothing, image super-

Presented by Medical*Online

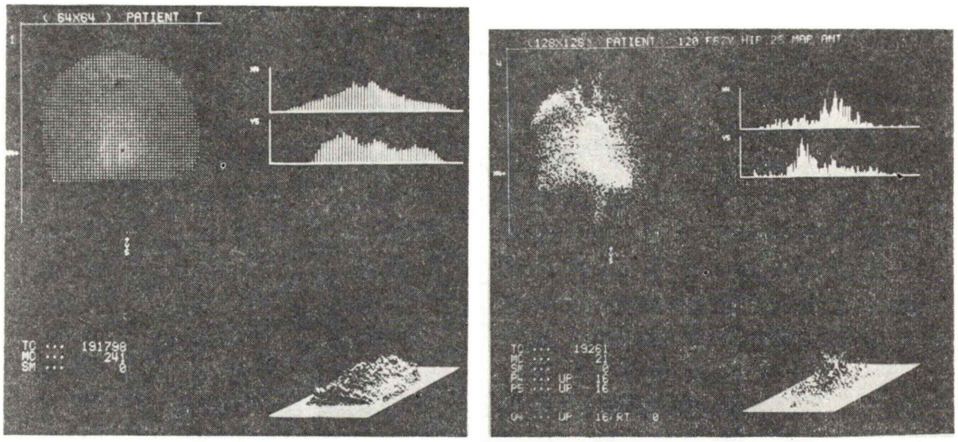

Fig. 9 Radioisotope image: profile and oblique display (30°).

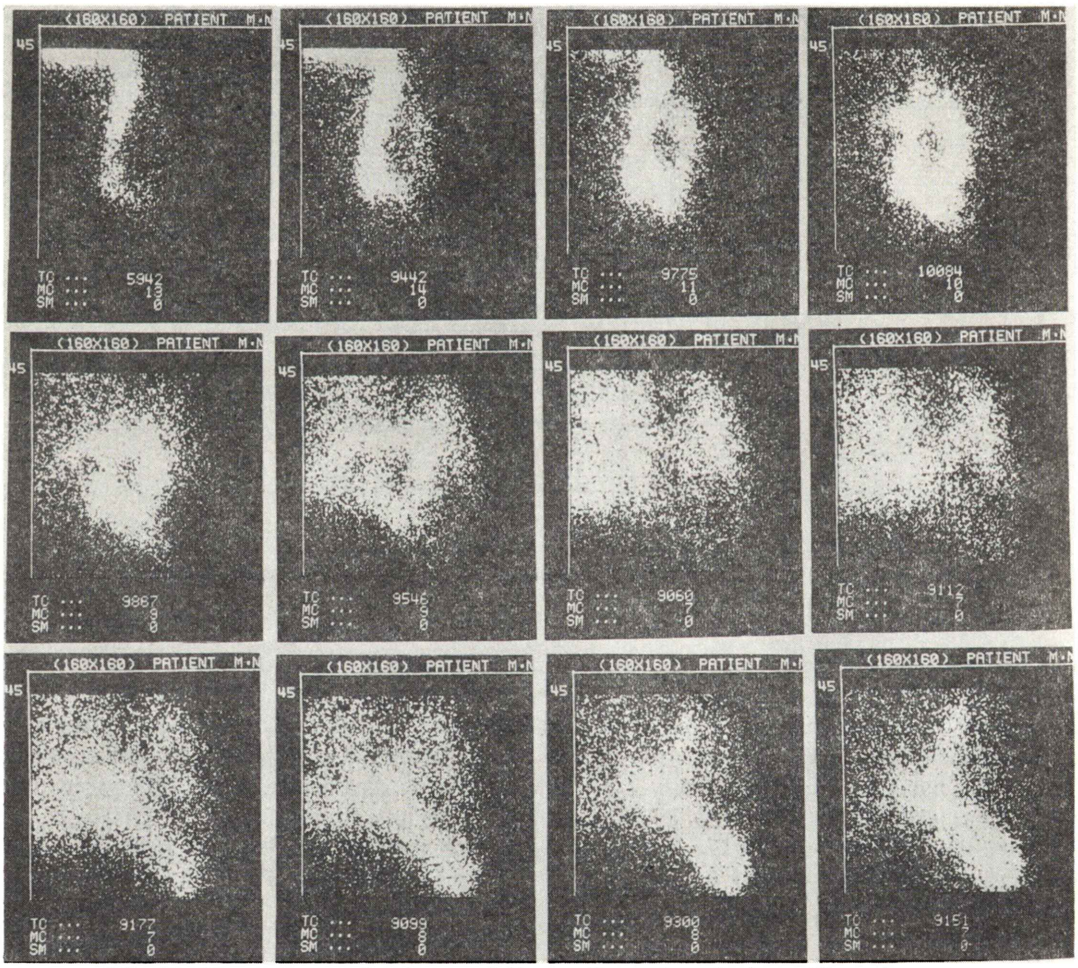

Fig. 10 80 msec composite pictures of 10 msec list mode gatherings with total counts, maximum counts, and smoothing readings.

Presented by Medical*Online

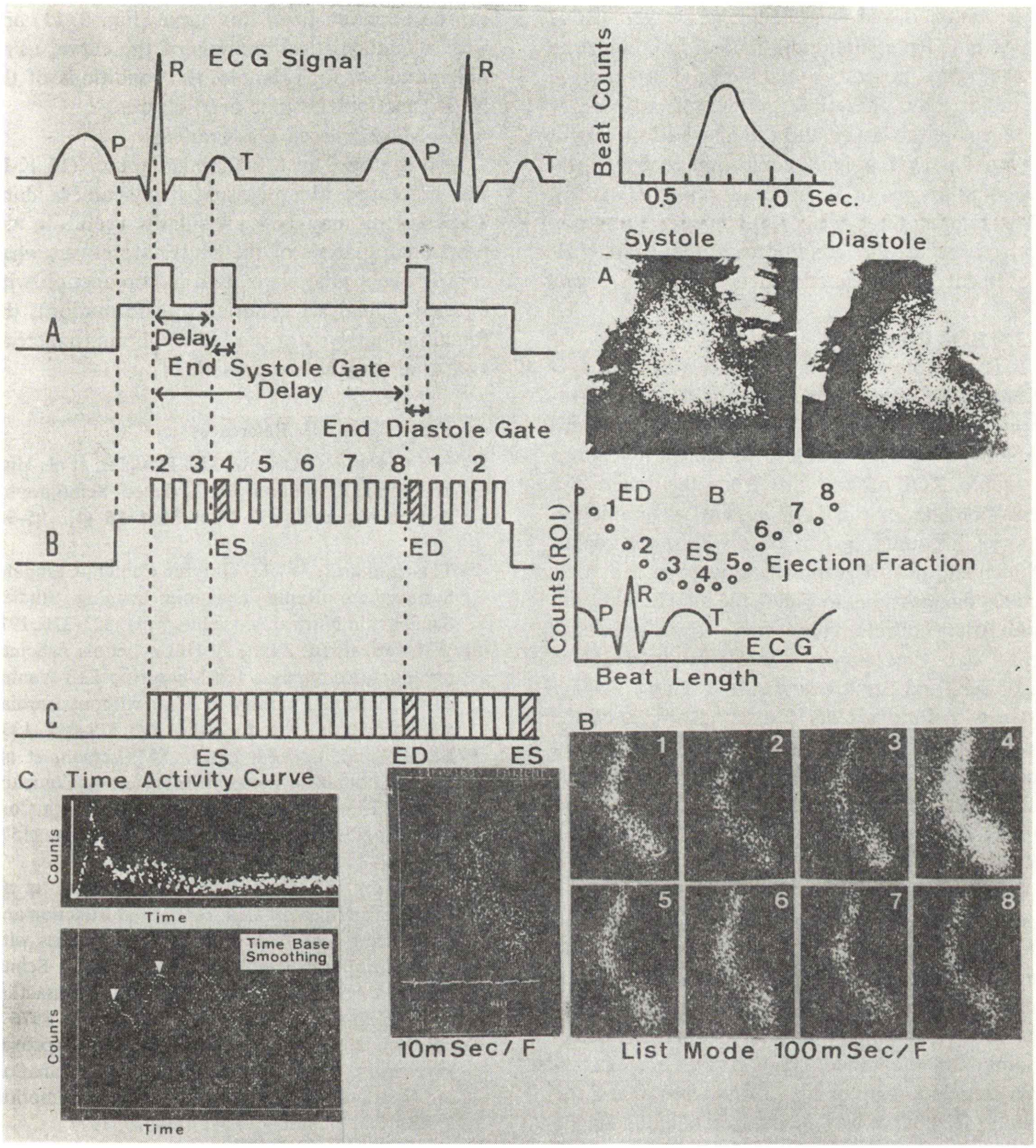

Fig. 11 ECG-gated method and list mode images:
(A) Two gated signal system and systole, diastole images.
(B) 1 beat units divided into equal gates providing data for 100 beat image accumulation IO curve.
(C) Equal interval gated image from which the ROI is decided and the IG curve is made.

imposing and ROI designation can be performed on all images, and for some images, profile display and oblique display are possible. Fig. 9 is an example of a display using data gathered by map mode with a profile display of the image. With an image using data gathered by list mode, it is

Presented by Medical*Online

possible to display organ image waves (ECG wave, blood pressure, etc.) concurrently with the image, add a point as a mark on the organ wave to indicate the phase the image depicts (in order to correlate the image and the phase of the organ wave), and get a high count image by superimposing images of a particular phase, (Fig. 10). By examining these images, it is possible to study such items as the condition of the heart wall movement or the functional image of an organ (Fig.11).

3. ROI Processing

It is possible to display the series of data collected in list mode concurrently with their corresponding ECG signals (four signal channels are possible) on a CRT and also to arbitrarily choose a square ROI of any size from the image the potentiometer of the LAB system, to graph the change in counts against time within the region of interest, and to graph the change in radiation activity against time. In Fig. 6, the interval between points (data collection time) was altered. The upper graph is a time/activity curve with intervals of 100 msec, and the lower graph is a time/activity curve with intervals of 10 msec. Analysis of the clearance curve, ejection fractions, functional image of the chambers, and count rate are possible using these curves. The maximum count was 256 in this study and the graph has been normalized by the maximum count.

4. On the IO IG Curves

Choosing a ROI and analyzing the change in counts within the ROI is a useful way to find the functional image of the organ. Data acquired by list mode was displayed in intervals of 10 msec and after choosing the region of interest, determining the clearance (IG) curve, and superimposing data from images in the same phase, the volume (IO) curve was determined (Fig. 6). In the case of the heart, analysis of the clearance curve will indicate interventricular defects, stroke volume, left ventricle volume, and its rate of change. The volume curve can be obtained by dividing each heart stroke into equal parts, superimposing images in the same phase, displaying the image of one stroke successively (Fig. 6, 11) choosing a ROI on the image, and graphing the change of counts within the ROI. The condition of various heart functions, such as the ejection fraction, can be observed from this curve (Fig. 6, 11) and with a mathematical analysis of the curve, using differentiation for example, the conditions of the heart functions become even clearer.

5. Miscellaneous Observations

In this study, an 8 bit minicomputer (16 K-B) was employed in processing the γ-camera data. This system may be particularly useful in the functional analysis of the heart. Moreover, when compartment analysis is used in conjunction with frequency analysis (Fourier transformation), the functional analysis of the kidney, brain, pancreas, and other organs are possible.

References

1) MV Green, HG Ostrow, MA Douglas, et al: High Temporal Resolution ECG Gated Scintigraphic Angiocardiography. J Nucl Med **16** (1): 95–98, 1975
2) TD Cradduck, WJ MacIntyre: Camera-Computer Systems for Rapid Dynamic Imaging Studies. Seminars in Nuclear Medicine. **7** (4): 323–336, 1977
3) WH Strauss, BL Zaret, PJ Hurley, et al: A Scintiphotographic Method for Measuring Left Ventricular Ejection Fraction in Man without Cardiac Catheterization. Am J Cardiol **28**: 575–580, 1977
4) ED Folland, GW Hamilton, SM Larson, et al: The Radionuclide Ejection Fraction: A Comparision of Three Radionuclide Techniques with Contrast Angiography. J Nucl Med **18** (12): 1157–1166, 1977
5) MV Green, SL Bacharach, MA Douglas, et al: The Measurement of Left Ventricular Function and the Detection of Wall Motion Abnormalities with High Temporal Resolution ECG Gated Scintigraphic Angiocardiography. IEEE Transaction on Nuclear Science **NS-23** (3): 1257–1263, 1976
6) ED Van Hove, LL Heck, JL Knight: Improved Myocardial Infarct Localization by Combination of Scintigraphy and Ventricular Wall/motion Evaluation. Radiology **124**: 425–429, 1977
7) SL Bacharach, MV Green, JS Borer, et al: A Real-Time System for Multi-Image Gated Cardiac Studies. J Nucl Med **18** (1): 79–84, 1977
8) WL Ashburn, HR Schelbert, JW Verba: Left Ventricular Ejection Fraction—A Review of Several Radionuclide Angiographic Approaches Using the Scintillation Camera, Principles of Cardiovascular Nuclear Medicine, edited by LB Holman, EH Sonnenblick, Michael Lesch: (Grune & Stratton Inc.), pp. 171–188, 1978
9) E Tobinik, HR Schelbert, H Henning, et al: Right

Presented by Medical*Online

Ventricular Ejection Fraction in Patients with Acute Anterior and Inferior Myocardial Infarction Assessed by Radionuclide Angiography. Circulation **57** (6): 1078–1084, 1978

10) JA Jengo, I Mena, A Blaufuss, et al: Evaluation of Left Ventricular Function (Ejection Fraction and Segmental Wall Motion) by Single Pass Radioisotope Angiography. Circulation **57** (2): 326–332, 1978
11) PJ Kenny, DD Watson, NR Zusmer, et al: Left Heart Imaging Following $C^{15}O_2$ Inhalation, IEEE Transactions on Nuclear. Science **NS-24** (No. 1): 563–566, 1977
12) HR Schelbert, JW Verba, AD Johnson, et al: Nontraumatic Determination of Left Ventricular Ejection Fraction by Radionuclide Angiocardiography. Circulation **51**: 902–909, 1975
13) DL Kirch, CE Metz, PP Steele: Quantitation of Valvular Insufficiency by Computerized Radionuclide Angiocardiography. Am J Cardio **34**: 711–721, 1974
14) WL Ashburn, HR Schelbert, G Brock, et al: Non invasive Measurement of Left-Ventricular Ejection Fraction, Nuclear Cardiology, Principle and Method, edited by AN Serafini, AJ Gilson, WM Smoak, (Plenum Medical Book Co.), pp. 171–178, 1976
15) RJ Nickles, PJ Nelson, RE Polcyn, et al: Radioactive Gases in the Evaluation of Left Ventricular Function, Nuclear Cardiology, Principle and Methods, edited by AN Serafini, AJ Gilson, WM Smoak, (Plenum Medical Book Co.) pp. 217–230, 1976
16) PJ Kenny, DD Watson, WR Janowitz, et al: The Use of $C^{15}O_2$ in the Evaluation of Cardiac Abnormalities, Nuclear Cardiology, Principle and Methods, edited by AJ Gilson, AN Serafini, WM Smoak (Plenum Medical Book Co.), pp. 303–215, 1976
17) RJ Nickles, JE Holden, AJ Kiuru, et al: Inclusion of Physiologic Data into Computerized Nuclear Medicine Dynamic Studies. J Nucl Med **17** (4): 297–300, 1976
18) D Twing, L Nardizzi, E Stokely: Parameter Estimation Applied to Noninvasive Radiocardiographic Data for Determination of Left Ventricular Ejection and Valvular Regurgitant Fractions, Mathematical Biociences (an International Journal). MABIAR **37** (1/2): 81–104, 1977
19) V Ullmann, V Husak, L Dubroka: Dead-Time Correction in Dynamic Radionuclide Studies by Computer. Eur J Nucl Med **3** (3): 197–202, 1978
20) T Iinuma, K Fukuhisa, T Matsumoto: Resolving Time of Scintillation Camera-Computer System and Methods of Correction for Counting Loss II On the Dynamic Performance of Various Types of Camera-Computer Systems. J S Nucl Med **12** (1): 25–32, 1975
21) JA Sorenson: Methods of Correction Anger Camera Deadtime Losses. J Nucl Med **17** (2): 137–141, 1976
22) JE Arnold, SA Johnston, SM Pinsky: The Influence of True Counting Rate and the Photopeak Fraction of Detected Events on Anger Camera Deadtime. J Nucl Med **15** (6): 412–416, 1974
23) R Wicks, M Blau: The Effect of Window Fraction on the Deadtime of Anger Camera: Concise Communication. J Nucl Med **18** (7): 732–735, 1977
24) S-E Strand, I Larsson: Image Artifacts at High Photon Fluence Rates in Single-Crystal NaI(Tl) Scintillation Cameras. J Nucl Med **19** (4): 407–413, 1978

Presented by Medical*Online

要　　旨

小型電算機による γ-Camera Data 処理
—ECG-Gate による心臓 Scintigram 動態機能に関する研究—

長谷川武夫*　赤木　清*　羽柴　広*　小林　昭智*
松田　孫一*　下釜　司**

*関西医科大学放射線科，**東芝メディカル株式会社システム技術科

われわれは Anger-type γ-Camera (GCA-202: Toshiba) と Tosbac-10E (Hospicon-600: Toshiba) の組み合わせによる心電同期の心動態機能解析の Software の開発を行なったので，その機能，性質について報告する．この方法は，Data を List Mode により 10 msec から 100 msec の任意の間隔で収集を行ない，同期して他の生体現象波の集収を行なう．従って同一 CRT 上に RI 画像と同期した生体現象を同時に表示し得るので，臨床上有用である．また，この方法の Deadtime は 40 μsec であり，従来の方法より大幅に deadtime を軽減できた．そのほか，種々の画像解析機能 (ROI 設定による IO, IG Courve の作成，Level Cut, Smoothing, Oblique 表示，Profil 表示，像の重ね合わせ) も臨床上有用であった．

Key words: Minicomputer, List Mode, RI Image, ECG-Gate

Presented by Medical*Online